Coherent backscattering cone shape depends on the beam size

Renzhe Bi, Jing Dong, and Kijoon Lee*

Division of Bioengineering, School of Chemical and Biomedical Engineering, Nanyang Technological University, 639798, Singapore

*Corresponding author: KJLee@ntu.edu.sg

Received 7 June 2012; revised 6 August 2012; accepted 8 August 2012; posted 9 August 2012 (Doc. ID 170165); published 5 September 2012

Coherent backscattering (CBS) is a beautiful physical phenomenon that takes place in a highly scattering medium, which has potential application in noninvasive optical property measurement. The current model that explains the CBS cone shape, however, assumes the incoming beam diameter is infinitely large compared to the transport length. In this paper, we evaluate the effect of a finite scalar light illumination area on the CBS cone, both theoretically and experimentally. The quantitative relationship between laser beam size and the CBS cone shape is established by using two different finite beam models (uniform top hat and Gaussian distribution). A series of experimental data with varying beam diameters is obtained for comparison with the theory. Our study shows the CBS cone shape begins to show distortion when beam size becomes submillimeter, and this effect should not be ignored in general. In biological tissue where a normal large beam CBS cone is too narrow for detection, this small beam CBS may be more advantageous for more accurate and higher resolution tissue characterization.

OCIS code: 030.1670, 290.1350.

1. Introduction

Coherent backscattering (CBS), also known as enhanced backscattering (EBS) or weak localization of photons [1,2], is a photon self-interference phenomenon which enhances the photon intensity in the backward direction of the incident light in the presence of highly scattering medium. From observation, a sharp cone always appears on top of the smooth diffuse background within a narrow angular distribution. The mathematical expression of this CBS cone was established in 1986 by using the time-reversal photon pairs model [3]. This phenomenon is observed in various scattering systems [4–7], and also discovered and studied in biological tissue [8,9].

The effect of partial coherence light source and low spatial coherence light source on a CBS cone was then studied [10–12]. Under such conditions, both theory and observation show that the full width at half-maximum (FWHM) of the CBS cone will increase and the enhancement factor of the CBS peak will be reduced. Because of these features, low-coherence enhanced backscattering (LEBS) has advantages in biological tissue characterization [13–16] where a normal CBS peak would be too narrow to observe. Relevant study suggests the reason behind LEBS cone shape is the elimination of photon pairs with high-order scattering events in the self-coherence signal [11,17–20].

For a CBS experiment, one typically uses a collimated laser beam with a diameter of several millimeters, which can be regarded as infinite illumination compared to ℓ^*, the transport mean free length of the medium. So the effect of finite illumination area has been ignored in most cases, until recent reports [21–24]. In this paper, we show this size effect exists even with a moderately small laser beam diameter, both theoretically and experimentally. The beam-size-induced distortion of a CBS cone is

1559-128X/12/266301-06$15.00/0

qualitatively similar to one by LEBS. We developed a new finite beam size CBS model based on the previous analysis by Akkermans, which is described in [3], to compare with our experimental data, and the simulation and experimental results show good correlation. The result indicates that we need to be very careful when the illumination beam diameter is in the submillimeter range, and the FWHM of a CBS cone can be broadened several times with a small illumination area. Thus, this phenomenon has high potential to help with facilitating the extremely narrow CBS cone detection, which is a main challenge for CBS application in biological tissue. The small beam size also means a smaller probing volume, which enables higher resolution mapping of optical properties.

2. Theory

The time-reversal photon pairs model is the most frequently used theory to explain the CBS phenomenon [3,8,11,25]. In this model, the coherent peak is regarded as an integration of all the constructively interfering photon pairs which share the same path but in an opposite direction, as shown in Fig. 1.

Under the assumption of infinite illumination area, the CBS peak can be described as [3]:

$$I(\theta) = \frac{3}{8\pi}\left[1 + \frac{2z_0}{\ell^*} + \frac{1}{(1 + k|\theta|\ell^*)^2}\left(1 + \frac{1 - \exp(-2z_0 k|\theta|)}{k|\theta|\ell^*}\right)\right]. \quad (1)$$

Where θ is the scattering angle from the exact backscattering direction, z_0 is extrapolation length that is given by [26,27]

$$z_0 = 2\ell^* \frac{1 + R_{\text{eff}}}{3(1 - R_{\text{eff}})}, \quad (2)$$

where $R_{\text{eff}} = -1.44/n^2 + 0.71/n + 0.668 + 0.064n$, n being the refractive index. When the refractive index is 1, $z_0 = 0.7\ell^*$, where ℓ^* is transport mean free path length. When θ is 0, the CBS cone reaches its maximum value, which is two times the background intensity. The ratio between maximum value and the background is the enhancement factor, which is 2 in theory. The enhancement factor does not change with ℓ^*, and the FWHM of the CBS cone is given by [28,29]

$$w = \frac{0.7\lambda}{2\pi\ell^*}. \quad (3)$$

However, in practice, we use a finite illumination area with a laser beam of several millimeters in diameter. To quantify the effect of the illumination area in CBS, we need to build a finite integration model over the illumination plane.

According to the CBS theory which was developed by Akkermans in 1986 [3], the backscattered albedo is then given by

$$\alpha(\mathbf{k}_i, \mathbf{k}_f) = (c/4\pi\ell^{*2}) \int \mathrm{d}z\mathrm{d}z'\mathrm{d}^2\rho \exp(-z/\mu_0\ell^*) \cdot \{1 + \cos[\mathbf{q}\cdot(\mathbf{r} - \mathbf{r}')]\} Q(\mathbf{r}, \mathbf{r}') \exp(-z'/\mu\ell^*), \quad (4)$$

where z and z' are the projections of $\mathbf{r}$ and $\mathbf{r}'$ on the z axis, ρ is the projection of $\mathbf{r} - \mathbf{r}'$ on the propagation plane, and μ_0 and μ are the directional cosines of $\mathbf{k}_i$ and $\mathbf{k}_f$ on the z axis, respectively. The factor $1 + \cos[\mathbf{q}\cdot(\mathbf{r} - \mathbf{r}')]$ is responsible for the interference. $Q(\mathbf{r}, \mathbf{r}')$ has been studied in classical transport theory, which is given by [27,30]

$$Q(\mathbf{r}, \mathbf{r}') = (1/4\pi D)\left(\frac{1}{|\mathbf{r} - \mathbf{r}'|} \frac{1}{(|\mathbf{r} - \mathbf{r}'|^2 + a^2)^{1/2}}\right), \quad (5)$$

where $a = 2(\ell^* + z_0)$. In a water-based liquid sample where the reflective index n is 1.33, $z_0 \approx 1.24\ell^*$.

Equation (1) has the integration over the x–y plane and z direction. The integration over the z direction is infinite, and can be easily done. The expression that is left only with ρ integration is given by

$$\alpha(\theta) = (3/4\pi^2\ell^*) \times \int \mathrm{d}^2\rho[1 + \cos(\mathbf{q}\cdot\boldsymbol{\rho})]\left(\frac{1}{\rho} - \frac{1}{(\rho^2 + a^2)^{1/2}}\right). \quad (6)$$

We transform this integration from the rectangular coordinate to polar coordinate, and can obtain

$$\alpha(\theta) = (3/4\pi^2\ell^*)\left[\int_0^{2\pi} \mathrm{d}\phi \int_0^R \left(\frac{1}{\rho} - \frac{1}{(\rho^2 + a^2)^{1/2}}\right)\rho\mathrm{d}\rho + \int_0^R \int_0^{2\pi} \cos(\mathbf{q}\cdot\boldsymbol{\rho})\left(\frac{1}{\rho} - \frac{1}{(\rho^2 + a^2)^{1/2}}\right)\rho\mathrm{d}\phi\mathrm{d}\rho\right]. \quad (7)$$

For the first term in the bracket, the $d\phi$ integration results in 2π, and for the second term in the bracket, the $d\phi$ integration results in $2\pi J_0(q\rho)$, where J_0 is the 0th order Bessel function of the first kind.

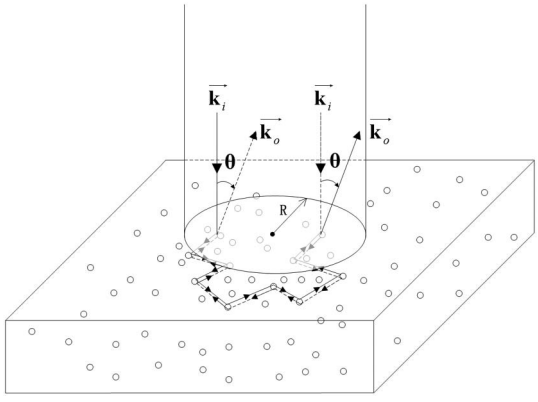

Fig. 1. Coherent multiple scattering inside a scattering medium. $\mathbf{k}_i$ is the incident wave vector and $\mathbf{k}_o$ is the emission wave vector, R is the radius of the beam.

$$\alpha(\theta) = (3/2\pi\ell^*)\Big[R + a - \sqrt{R^2 + a^2} + \int_0^R J_0(q\rho)\mathrm{d}\rho - \int_0^R J_0(q\rho)\frac{\rho}{(\rho^2 + a^2)^{1/2}}\mathrm{d}\rho\Big], \quad (8)$$

where $q = 2\pi|\theta|/\lambda$, and R is the radius of the light beam.

Equation (8) gives us the CBS peak profile under finite illumination conditions, with the light beam radius of R. This result so far is based on uniform illumination within the light beam. However, the practical laser beam is better approximated as a Gaussian beam, whose intensity distribution follows Gaussian function in its propagating plane. Then we need to modify Eq. (4) for better simulation.

$$\alpha(\mathbf{k}_i, \mathbf{k}_f) = (c/4\pi\ell^{*2}) \int \mathrm{d}z\mathrm{d}z'\mathrm{d}^2\rho \exp(-z/\mu_0\ell^*) \cdot \{1 + \cos[\mathbf{q}\cdot(\mathbf{r} - \mathbf{r}')]\}Q(\mathbf{r}, \mathbf{r}') \times \exp(-z'/\mu\ell^*)\exp(-2\rho^2/R^2), \quad (9)$$

where we assume the intensity of the Gaussian beam drops by $1/e^2$ at radius R. This integration range reaches infinity and can only be calculated numerically.

3. Experiment Methods

The schematic of our experiment setup is shown in Fig. 2. We use a diode laser working at 655 nm (Melles Griot, 56ICS254/HS). Right after the laser source, a neutral density filter is employed to reduce the light intensity. Then the laser beam is expanded by two biconvex lenses to 6 mm in diameter, and we use a small pinhole in front of the beam splitter to control the beam size. Then, a 50:50 nonpolarizing beam splitter guides the laser beam incident into the sample, which is tilted slightly to avoid the specular reflection. The distance between the pinhole and the sample surface is 5.5 cm, and in the directly backward direction, the backscattered signal is collected by a lens of 100 mm focus length. A CCD (Photometrics, Cascade 512F) with the pixel size of 16×16 μm is placed in the focal plane of the lens.

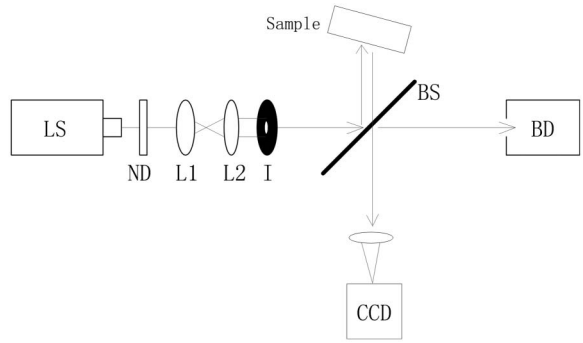

Fig. 2. Schematic of experimental setup for CBS cone measurement. LS is laser source, ND is neutral density filter, L1 and L2 are lenses, I is iris, BS is beam splitter, BD is beam dump.

We use a commercial brand intralipid (BBraun, Lipofundin N 20%) which is a highly scattering liquid medium as a sample. By using different pinholes of different sizes, we generate a series of laser beams with varying diameters. For image acquisition, 20 images are taken for average at certain diameter, and the exposure time is set between 0.1–1 s for optimal use of dynamic range.

4. Results

To validate that we indeed observe the CBS cone, we first used a 6 mm diameter laser beam to get a series of CBS images from samples with different concentrations of scatterers. For samples, we diluted the intralipid with water, so that the concentrations change from 90% to 30%, by steps of 10%. From Eq. (2), the reduced scattering coefficient μ_s' can be calculated from the FWHM of CBS cone. The linear relationship between concentration and μ_s' is shown in Fig. 3. This μ_s' value again was validated by separate optical measurement using frequency-domain diffuse optical spectroscopy.

Then we placed the pinhole in front of the beam splitter, with diameters of 138, 262, 369, 554, 692, and 1025 μm. 60% intralipid is used as a sample, where the μ_s' calculated from FWHM of the CBS cone is 221 cm^{-1}. Our normalized experimental CBS profiles are shown in Fig. 4. As beam diameter becomes

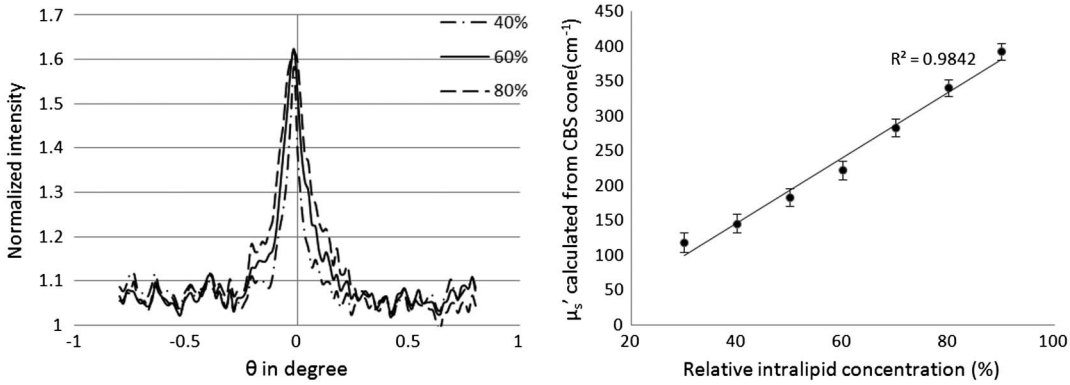

Fig. 3. (Left) CBS cones of different intralipid concentrations, and (right) relationship between intralipid concentration and μ_s' calculated from FWHM.

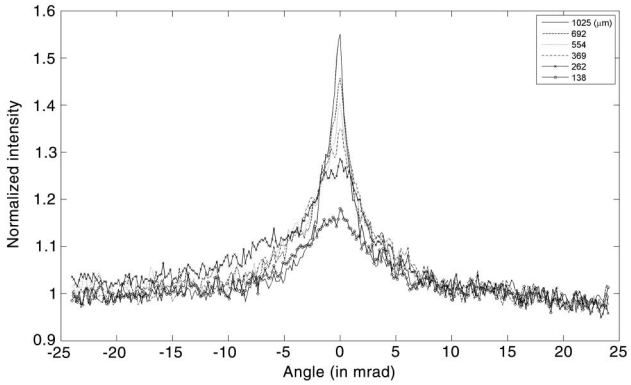

Fig. 4. Experimental CBS profiles with different beam sizes.

smaller, the CBS cone will become broader and lower, in a similar fashion as the LEBS cone behaves.

To compare with experimental data, the simulation result from Eq. (8) with the same set of beam diameters is shown in Fig. 5. We do the integration over ρ numerically, using a trapezoidal integration method. The integration range is from 0 to R, which is the radius of the laser beam.

We compare the FWHM and enhancement factor between experimental data and simulation data with finite uniform illumination and Gaussian illumination in Fig. 6.

From Fig. 6, the FWHM of the CBS cone will become broader and enhancement factor will drop when the incident light beam size decreases. For FWHM, though both simulations of uniform illumination and Gaussian illumination show the same trend as the experimental data, the experimental result fits the Gaussian beam simulation much better. In the submillimeter range, FWHM of experimental and simulated CBS cones are comparable. However, they start to deviate from each other as beam size becomes even smaller. For enhancement factor, Fig. 6(b) shows the decreasing trend of enhancement factor as beam diameter becomes smaller, both theoretically and experimentally. However, due to experiment limitation, theoretical and experimental enhancement factors do not match well in their absolute values. The result from Fig. 6 implies the measurement of CBS cone width may not be accurate when a small illumination area is used. A recent simulation study [24] also shows the same trend in an even smaller illumination area, where a Gaussian beam waist is applied.

From the viewpoint of the time-reversal photon pairs model, when a small beam size is used, the photon pairs sharing the same path with longer end-to-end spatial distance than the beam diameter in an x–y plane cannot contribute to the coherent part of albedo. As a result, most of the long path length photon pairs are excluded from the CBS cone, and the FWHM will become larger and enhancement factor will drop. Our result provides a quantitative relationship between illumination beam size and the CBS cone shape.

5. Discussion and Conclusion

In Fig. 6, FWHM of the smallest beam diameter shows the largest deviation between theoretical and experimental data, and the experimental data is much smaller than the theoretical prediction. This may be caused by the diffraction effect. Under our experimental condition, for the 138 μm diameter pinhole, the airy disk diameter at the distance used in our experimental setup is about 500 μm, which is a significant source of error in comparison. For other, bigger pinholes, the diffraction effect can be neglected. Also as the beam diameter becomes smaller, the SNR will drop because total photon number drops, which explains the larger error bars for smaller beam diameter in Fig. 6.

Because of our instrument's limitation, the enhancement factor cannot reach the ideal value 2, and it drops a bit faster than the theory predicts. Because of the width of the CCD pixel, our measurement is the convolution of the real signal and CCD spatial response function. Thus, enhancement factor is practically more sensitive to experimental conditions than FWHM, and it makes more sense to study FWHM of the CBS cone.

If the laser beam diameter can be constrained even smaller, so that it is comparable to ℓ^*, only photon pairs which experience double scattering events

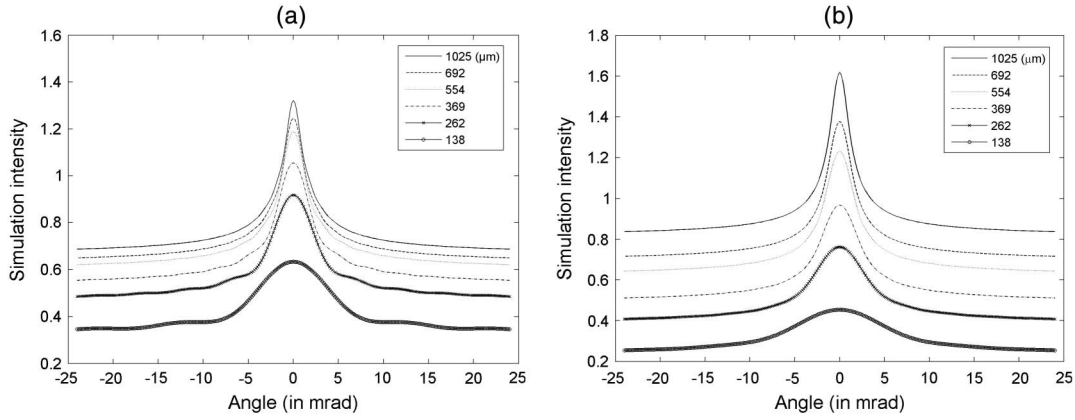

Fig. 5. Simulated CBS profiles with different beam sizes. (a) is uniform illumination and (b) is Gaussian beam illumination.

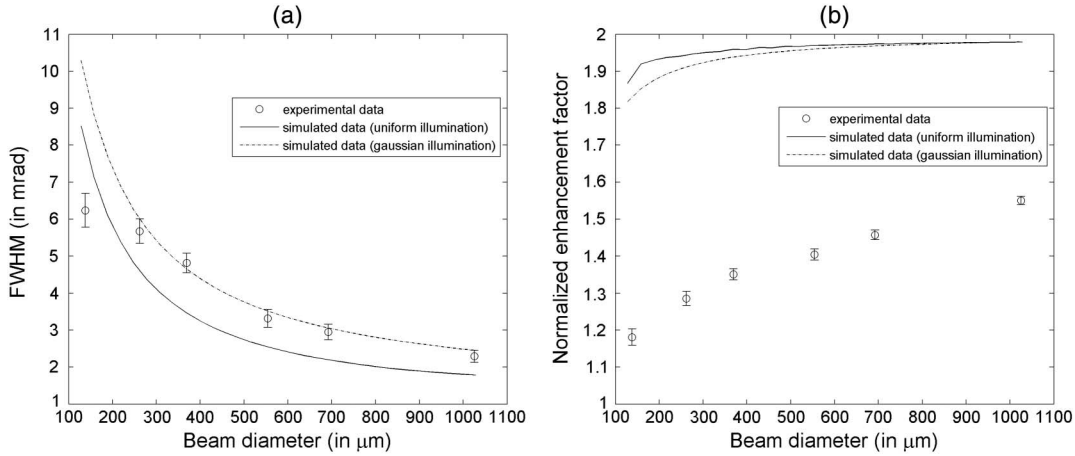

Fig. 6. Comparison of (a) FWHM and (b) enhancement factor of a CBS cone with varying beam sizes: among experimental data, simulation of finite uniform illumination, and Gaussian illumination.

can contribute to the CBS cone, then this small beam size CBS cone is a LEBS cone in nature. However, such a narrow laser beam is difficult to achieve.

In conclusion, we quantitatively studied the relationship between illumination area and CBS cone, and showed that the FWHM broadens and enhancement factor decreases as the beam size becomes smaller. Simulation results of two types of finite illumination are demonstrated to compare with experimental CBS data. For experimental conditions with a small size collimated laser beam or focused beam with small width, we should take beam size effect into consideration by using the finite integration method. This small beam size effect shows a significantly broader CBS cone, with high potential to be applied in biological tissue study, where the narrow CBS angular profile remains a great challenge.

Furthermore, every imaging modality that uses a coherent light source in epiluminal geometry, such as OCT or confocal microscopy, should inherently have a CBS phenomenon associated with the signal. Although the shape of the CBS cone may be too broad to be treated as significant, there surely exists the effect of CBS on each imaging modality that will have to be understood and compensated for. We are working on extending our current study in order to assess the CBS effect in an OCT signal, with a goal of improving OCT image quality with help from a CBS cone width measurement.

This work is supported by the Singapore Ministry of Education under the Academic Research Fund Tier 1 grant RG37/07. We are thankful for useful input by Dr. Mishchenko and kind support from Prof. Yoonhee.

References

1. P. E. Wolf and G. Maret, "Weak localization and coherent backscattering of photons in disordered media," Phys. Rev. Lett. **55**, 2696–2699 (1985).
2. M. P. Van Albada and A. Lagendijk, "Observation of weak localization of light in a random medium," Phys. Rev. Lett. **55**, 2692–2695 (1985).
3. E. Akkermans, P. E. Wolf, and R. Maynard, "Coherent backscattering of light by disordered media—analysis of the peak line-shape," Phys. Rev. Lett. **56**, 1471–1474 (1986).
4. G. Labeyrie, C. A. Muller, D. S. Wiersma, C. Miniatura, and R. Kaiser, "Observation of coherent backscattering of light by cold atoms," J. Opt. B **2**, 672–685 (2000).
5. R. Sapienza, S. Mujumdar, C. Cheung, A. G. Yodh, and D. Wiersma, "Anisotropic weak localization of light," Phys. Rev. Lett. **92**, 033903 (2004).
6. D. V. Kupriyanov, I. M. Sokolov, C. I. Sukenik, and M. D. Havey, "Coherent backscattering of light from ultracold and optically dense atomic ensembles," Laser Phys. Lett. **3**, 223–243 (2006).
7. P. C. DeOliveira, A. E. Perkins, and N. M. Lawandy, "Coherent backscattering from high-gain scattering media," Opt. Lett. **21**, 1685–1687 (1996).
8. K. M. Yoo, G. C. Tang, and R. R. Alfano, "Coherent backscattering of light from biological tissues," Appl. Opt. **29**, 3237–3239 (1990).
9. G. Yoon, D. N. Roy, and R. C. Straight, "Coherent backscattering in biological media: measurement and estimation of optical properties," Appl. Opt. **32**, 580–585 (1993).
10. T. Okamoto and T. Asakura, "Enhanced backscattering of partially coherent light," Opt. Lett. **21**, 369–371 (1996).
11. Y. L. Kim, P. Pradhan, H. Subramanian, Y. Liu, M. H. Kim, and V. Backman, "Origin of low-coherence enhanced backscattering," Opt. Lett. **31**, 1459–1461 (2006).
12. M. Tomita and H. Ikari, "Influence of finite coherence length of incoming light on enhanced backscattering," Phys. Rev. B **43**, 3716–3719 (1991).
13. Y. L. Kim, Y. Liu, R. K. Wali, H. K. Roy, and V. Backman, "Low-coherent backscattering spectroscopy for tissue characterization," Appl. Opt. **44**, 366–377 (2005).
14. V. Turzhitsky, A. J. Radosevich, J. D. Rogers, N. N. Mutyal, and V. Backman, "Measurement of optical scattering properties with low-coherence enhanced backscattering spectroscopy," J. Biomed. Opt. **16**, 067007 (2011).
15. Y. L. Kim, V. M. Turzhitsky, Y. Liu, H. K. Roy, R. K. Wali, H. Subramanian, P. Pradhan, and V. Backman, "Low-coherence enhanced backscattering: review of principles and applications for colon cancer screening," J. Biomed. Opt. **11**, 041125 (2006).
16. J. J. Liu, Z. B. Xu, Q. H. Song, R. L. Konger, and Y. L. Kim, "Enhancement factor in low-coherence enhanced backscattering and its applications for characterizing experimental skin carcinogenesis," J. Biomed. Opt. **15**, 037011 (2010).
17. M. Xu, "Low-coherence enhanced backscattering beyond diffusion," Opt. Lett. **33**, 1246–1248 (2008).
18. H. Subramanian, P. Pradhan, Y. L. Kim, Y. Liu, X. Li, and V. Backman, "Modeling low-coherence enhanced backscattering

using Monte Carlo simulation," Appl. Opt. **45**, 6292–6300 (2006).
19. V. Turzhitsky, J. D. Rogers, N. N. Mutyal, H. K. Roy, and V. Backman, "Characterization of light transport in scattering media at subdiffusion length scales with low-coherence enhanced backscattering," IEEE J. Sel. Top. Quantum Electron. **16**, 619–626 (2010).
20. V. Turzhitsky, N. N. Mutyal, A. J. Radosevich, and V. Backman, "Multiple scattering model for the penetration depth of low-coherence enhanced backscattering," J. Biomed. Opt. **16**, 097006 (2011).
21. V. Turzhitsky, A. Radosevich, J. D. Rogers, A. Taflove, and V. Backman, "A predictive model of backscattering at subdiffusion length scales," Biomed. Opt. Express **1**, 1034–1046 (2010).
22. A. J. Radosevich, N. N. Mutyal, V. Turzhitsky, J. D. Rogers, J. Yi, A. Taflove, and V. Backman, "Measurement of the spatial backscattering impulse-response at short length scales with polarized enhanced backscattering," Opt. Lett. **36**, 4737–4739 (2011).
23. A. J. Radosevich, J. D. Rogers, V. Turzhitsky, N. N. Mutyal, J. Yi, H. K. Roy, and V. Backman, "Polarized enhanced backscattering spectroscopy for characterization of biological tissues at subdiffusion length scales," IEEE J. Sel. Top. Quantum Electron. **18**, 1313–1325 (2012).
24. D. W. Mackowski and M. I. Mishchenko, "Direct simulation of multiple scattering by discrete random media illuminated by Gaussian beams," Phys. Rev. A **83**, 013804 (2011).
25. E. Akkermans, P. E. Wolf, R. Maynard, and G. Maret, "Theoretical-study of the coherent backscattering of light by disordered media," J. Phys. (Paris) **49**, 77–98 (1988).
26. R. C. Haskell, L. O. Svaasand, T. T. Tsay, T. C. Feng, and M. S. McAdams, "Boundary-conditions for the diffusion equation in radiative-transfer," J. Opt. Soc. Am. A **11**, 2727–2741 (1994).
27. T. Durduran, R. Choe, W. B. Baker, and A. G. Yodh, "Diffuse optics for tissue monitoring and tomography," Rep. Prog. Phys. **73**, 076701 (2010).
28. P. E. Wolf, G. Maret, E. Akkermans, and R. Maynard, "Optical coherent backscattering by random-media—an experimental-study," J. Phys. (Paris) **49**, 63–75 (1988).
29. Y. L. Kim, Y. Liu, V. M. Turzhitsky, H. K. Roy, R. K. Wali, and V. Backman, "Coherent backscattering spectroscopy," Opt. Lett. **29**, 1906–1908 (2004).
30. J. B. Fishkin and E. Gratton, "Propagation of photon-density waves in strongly scattering media containing an absorbing semiinfinite plane bounded by a straight edge," J. Opt. Soc. Am. A **10**, 127–140 (1993).